Measurement of Some Basic Parameters in Two-Phase Annular Flow

E. R. QUANDT

United States Navy, Marine Engineering Laboratory, Annapolis, Maryland

The vertical upflow of air-water mixtures in the dispersed-annular flow regime has been studied in a ¼ × 3-in. rectangular channel. Dye injection into the wall film was used to determine film and gas core properties along with the rate of droplet interchange between the core and the film. Visual observations demonstrated that the most important characteristic of this flow regime is the surface waves generated by the gas flow over the liquid film. Despite the surface waves, these data indicate that the liquid film approximately follows the generalized $u^+ - y^+$ relationship for turbulent pipe flow. The droplet motion is discussed in terms of transverse diffusion and momentum transfer.

The simultaneous flow of gas and liquid phases is a commonly observed and highly attractive process. Industrial applications range from boilers and condensers to film contactors and spray dryers. In a much larger sense, the natural motion of air currents over large bodies of water is of great significance in determining weather and climate. Whatever the scale of the process, in order to understand and control two-phase behavior one needs to know something about the interfacial heat, mass, and momentum transfer properties. Engineering analyses typically begin with the assumption that the gas-liquid interfaces are smooth surfaces, and deviations from predictions are frequently attributed to waves or ripples which develop at the interface. In some cases the deviations may be small, while in others the surface effects may be such a significant part of the problem that the waves must be considered. The present understanding of wind-wave generation is given by Lighthill (*1*), while some indication of the application to engineering systems is reported by Hanratty and Hershman (*2*) in their study of roll waves.

The purpose of this paper is to present a set of internal experimental data for the annular two-phase flow regime. Herein annular flow is assumed to include what are often called annular, spray annular, dispersed, fog, and mist types of two-phase flow (*3, 4*). The single term *annular flow* is used since it is felt that there is normally a liquid film on the channel walls for each of these flow regimes. Moreover, from an experimental standpoint the surface waves generated on this film seem to be of vital importance to the whole process. However, owing to the analytical complexity, the surface wave problem will not be pursued, except in the sense that the data has been handled in a manner felt to be compatible with a surface wave model.

Much of the previous work in the two-phase annular flow regime has been concerned with experimental studies of the heat, mass, and momentum transfer characteristics of steam-water mixtures. It has become apparent from the heat transfer investigations that boiling, for example, in the annular flow regime differs markedly from other types of boiling in that vapor bubbles are not observed on the heating surfaces (*5, 6*). This observation implies that heat removal in annular flow is accomplished by a more efficient surface vaporization of the wavy liquid film. Burnout in this regime must then be closely related to a drying up of the liquid film as observed by Kinney, Abramson, and Sloop (*7*) in their experiments on the film cooling of rocket nozzles. Analytical models for burnout would be similar to those proposed by Isbin, Vanderwater, Fauske, and Singh (*8*), by Goldman, Firstenberg, and Lombardi (*9*), and by Silvestri (*10*).

A vast amount of momentum transfer, or pressure drop, information concerning two-phase annular flow is also available in the literature. Perhaps the most well-known treatment is the empirical gas fraction and frictional pressure drop correlations of Martinelli and Nelson (*11*). These results are based only upon a knowledge of the separate gas and liquid flow rates, the physical properties, and the channel geometry. Following the publication of these general correlations, an improved understanding of the underlying physical principles has gradually developed. Collier and Hewitt (*12*) have reported measurements of film thickness, entrainment, and pressure drop for the vertical flow of air-water mixtures. Dukler and Magiros (*13*) presented measurements of entrainment and pressure drop for horizontal air-water flow. Van Rossum (*14*) has investigated the wave formation, atomization characteristics, and thicknesses of horizontal liquid films. Bankoff (*15*) and Levy (*16*) have developed analytical models of two-phase turbulent flow by considering the gas and liquid to form a homogeneous fluid with variable properties across the flow channel. Other analytical models based upon a distinct liquid film on the channel walls have been proposed by Calvert and Williams (*17*) and by Dukler (*18*). As mentioned previously, Hanratty and Hershman (*2*) have reported both experimental data and an analysis on the initiation of roll waves in the horizontal flow of liquid films. Worthwhile surveys of the current understanding of two-phase annular flow have been written by Lacey, Hewitt, and Collier (*19*) from Harwell and by those working on the CAN project for Euratom (*20*).

THEORY

Figure 1 illustrates the relatively simple physical model which has been assumed to describe two-phase annular

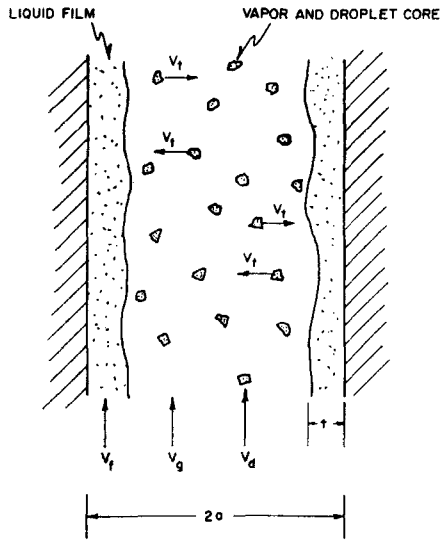

Fig. 1. Physical model of annular flow.

flow between two infinitely wide parallel plates a distance $2a$ apart. The liquid film is considered to be defined by an average thickness t and an average velocity V_f. The gas-droplet core is characterized by an average gas velocity V_g and by an average axial droplet velocity V_d. A second component of the droplet velocity V_t has been defined at the film-core interface to account for the rate of droplet transfer to the liquid film and also for the subsequent re-entrainment. (In a steady state condition the average droplet mass transfer to the film must be equal to the transfer from the film so that a single value of V_t is sufficient for the present purposes.) It is felt that this cross-flow velocity term is significant in two-phase annular flow since it accounts for a certain part of the mass and momentum transfer.

The general problem to be investigated with this flow model is: given the total liquid and gas flow rates, the channel spacing, and the physical properties of each phase, what are the corresponding values of V_f, t, V_d, V_t, and V_g? The experimental technique used to evaluate these variables was based on dye injection into the liquid film on the channel walls. It is assumed that the amount of dye injected is negligible with respect to the total flow of liquid on the wall and that the dye is injected uniformly on both sides of the channel and across the complete flow width. It is also assumed that at any axial position the dye concentration is uniform across the width and thickness of the film and that the droplet dye concentration in the gas-droplet core is uniform across the width and thickness of the core. Hence, if dye is injected continuously into the liquid film at some axial position, and the concentration of dye in the film is measured at subsequent axial positions, the film concentration should decrease with distance along the channel because of mass transfer with the originally colorless droplets in the gas-droplet core.

The rate of decrease of film concentration may be expressed in terms of the quantities defined in Figure 1 so that measurement of this variation will permit evaluation of certain of the basic parameters. Making a mass balance on the dye for a differential length of liquid film at some axial position one gets

$$\left[\frac{V_f t}{V_t(1-R_{go})}\right]\frac{dC_f}{dz} = C_d - C_f \qquad (1)$$

A complementary relationship may be obtained for the liquid droplet concentration by again making a dye mass balance on the gas-droplet core

$$\left[\frac{V_d(a-t)}{V_t}\right]\frac{dC_d}{dz} = C_f - C_d \qquad (2)$$

Equations (1) and (2) may be solved simultaneously from the boundary condition that at $z = 0$, $C_f = C_o$, and $C_d = 0$. This solution yields the following equations for film and droplet dye concentration as functions of distance from the point of dye injection

$$\left(\frac{C_f}{C_o}\right)(z) = 1 + E\,(e^{-kz} - 1) \qquad (3)$$

$$\left(\frac{C_d}{C_o}\right)(z) = (1-E)\,(1-e^{-kz}) \qquad (4)$$

where

$$k = \frac{V_t(1-R_{go})}{V_f\,t\,E} = \frac{G_t}{p_f V_f\,t\,E} \qquad (5)$$

Here E is defined as the fraction of liquid flowing as entrained droplets. It can be seen that as $z \to \infty$ the film and droplet concentrations become equal at some value of dye concentration, say C_m. In an experiment on two-phase flow it is more convenient to express the film concentration in terms of C_m rather than C_o, since C_o is, in general, difficult to measure. C_m may be measured quite easily by collecting and mixing all of the liquid after it has passed through the channel. Equation (6) thus gives the film concentration in terms of C_m, E and k

$$\left(\frac{C_f}{C_m}(z) - 1\right) = \frac{E}{1-E}\,e^{-kz} \qquad (6)$$

Data reduction is accomplished by plotting the left-hand side of (6) vs. distance on semi-log paper. Entrainment E is given by the intercept at $Z = 0$, while the interchange constant k is found from the slope. Evaluation of G_t is possible from Equation (5), wherein it may be noted that the grouping $\rho_f V_f t$ is equivalent to the film mass flow per unit wetted perimeter, that is $(1 - E)W_t/2(L + 2a)$. Thus G_t is determined by the film concentration variation, the entrainment, and the total liquid flow. Using the total liquid peripheral flow and the measured film velocity one can also compute film thickness t. Gas core liquid fraction $(1 - R_{go})$ is found by subtracting the film volume from the total measured liquid fraction and finally droplet velocity from the $(1 - R_{go})$ and the entrainment. In general this procedure appeared satisfactory, the data scatter being less than 25% and the trends of several groups being similar.

The physical model of two-phase annular flow presented in Figure 1 allows a rather detailed investigation of two-phase pressure drop. In particular, it is evident that the total drag, or frictional resistance, for this type of flow regime must arise because of a difference in velocity between the liquid film and the channel walls. This drag is transmitted to the gas core by a droplet transfer mechanism in addition to the usual single phase gas turbulent transfer. The following equations are derived in order to clarify the phenomena involved and to aid in computation of the pressure drop resulting from this type of flow.

Writing the law of conservation of momentum for steady flow through an arbitrarily shaped, but fixed, control volume $\mathcal{V}$ with surface S one obtains the following integral equation

$$\frac{1}{g_c}\int_s (\vec{\rho V})\,\vec{V}\cdot\vec{dS} = \int_s \vec{p}\,dS + \int_v \frac{\vec{g}}{g_c}\,d\mathcal{V} \qquad (7)$$

In order to evaluate these vector quantities, let the unit vector $\vec{j}$ be in the direction of flow and the unit vector $\vec{i}$

be normal to flow direction and into the channel wall on the right-hand side of Figure 1. It is also necessary to define the shear stress on the channel walls by τ_w and the gas-liquid shear stress in the absence of droplet transfer by τ_f.

Considering a volume of differential length dz for the gas-droplet core one gets the following physical picture

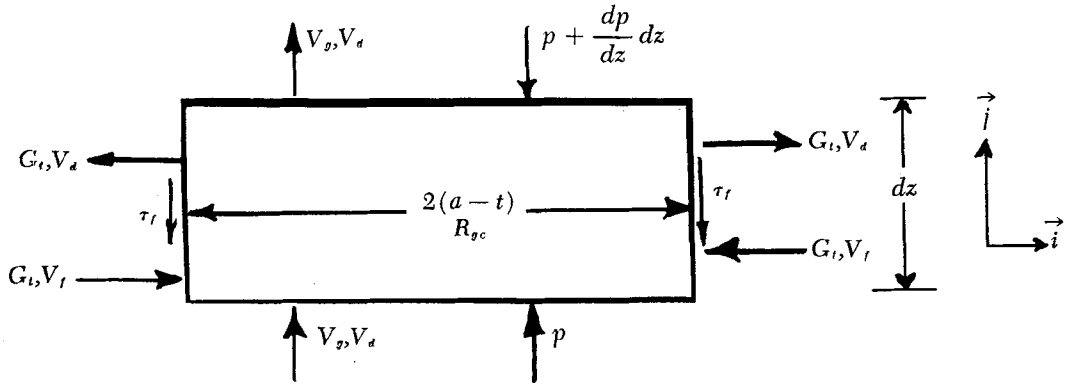

The individual components of the integral momentum balance may now be written as follows for vertical upflow, with negligible density changes assumed

$$\int_s \vec{p}\, dS = -\vec{j} \frac{dp}{dz} (2a - 2t)\, dzL - \vec{j}\, 2\tau_f L dz \quad (8)$$

$$\int \rho \frac{g}{g_c} d\mathcal{V} = -\vec{j} \left[\rho_g R_{gc} + \rho_f (1 - R_{gc})\right] 2 (a - t)\, L\, dz \quad (9)$$

$$\frac{1}{g_c} \int_s (\vec{\rho V}) \vec{V} \cdot \vec{dS} = \frac{\vec{j}}{g_c} \left[2V_d - 2V_f\right] \rho_f V_t (1 - R_{gc}) L\, dz \quad (10)$$

Combining Equations (8), (9), and (10) one obtains an expression for the pressure drop in the gas-droplet core

$$-\frac{dp}{dz} = \frac{G_t}{(a-t)g_c} (V_d - V_f) + \frac{\tau_f}{(a-t)} + \left[\rho_g R_{gc} + \rho_f (1 - R_{gc})\right] \quad (11)$$

Performing similar computations for the liquid film results in the following equation for the pressure gradient in the liquid film

$$-\frac{dp}{dz} = -\frac{G_t}{tg_c} (V_d - V_f) - \frac{\tau_{ft}}{t} + \frac{\tau_w}{t} + \rho_f = -\frac{\tau_{ft}}{t} + \frac{\tau_w}{t} + \rho_f \quad (12)$$

Here τ_{ft} is the total interfacial shear stress, including the droplet momentum interchange term. Finally, it is also valuable to show the pressure gradient with the complete channel width as a control volume

$$-\frac{dp}{dz} = \frac{\tau_w}{a} + \rho_g R_{gt} + \rho_f (1 - R_{gt}) \quad (13)$$

It is interesting to note that at very high gas fractions the overall pressure gradient is primarily a function of the wall shear stress τ_w. For high gas fractions the liquid films are quite thin, so that the wall shear stress is determined mainly by τ_f and $G_t/g_c\ (V_d - V_f)$. If the cross flow mass velocity is high and the droplets move much faster than the film, then the wall shear stress and consequent frictional loss will be large. Also, if total pressure gradient is measured, it will be possible to obtain additional information about τ_f, the shear stress at the gas-liquid interface arising from turbulence in the gas-droplet core.

EXPERIMENT

Description of Equipment

The test section used in these experiments was an 8 ft. long rectangular channel having internal dimensions of ¼ × 3 in. A cross-sectional view of the construction is given in Figure 2*a*. The entire unit was fabricated from Plexiglas so that a dye-injection and photocell technique could be used to measure the film velocity and also to permit direct visual observation of the behavior of the two phases. As shown in the figure, the corner regions were designed to provide an undistorted view of the flow in the channel corners. Rubber 0-ring seals were used to prevent leakage around the mating surfaces between the edge spacers and the front plates. The complete assembly was bolted together through the edge spacers with aluminum angles as a support. Cross pieces spanned the channel width to assure a uniform plate spacing of ¼ in.

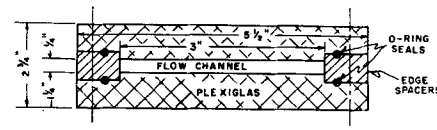

Fig. 2*a*. Cross section of annular flow study test section.

Annular flow was established by introducing the air directly into the bottom of the channel while the water was injected uniformly onto the channel walls through two porous stainless steel plates on opposite sides of the channel. Each porous plate, 0.0025 in. pore size, extended over the entire length of the 3-in. side of the channel and was located 2 in. from the inlet. These plates were recessed into the walls so that the inside surface of the channel was continuous and smooth. It was felt that injection of the liquid uniformly on the walls through these small pores was the most desirable for establish-

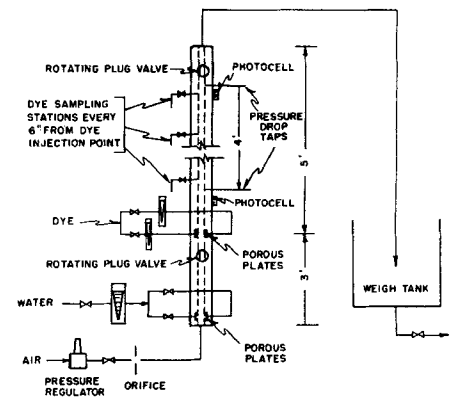

Fig. 2*b*. Schematic of annular flow study test apparatus.

ing annular flow since any excess liquid in the film would be quickly entrained to form spray. To permit equilibrium to occur between the droplets and the film the bottom 3-ft. length was considered as an inlet length, and measurements were restricted to the upper 5 ft. of the channel.

Figure 2*b* shows the overall flow paths and instrumentation arrangements used for this experiment. The air flow rate was measured with a sharp edged orifice, and the water rate was determined by collecting and weighing the total amount of water which passed through the channel. Orifice pressure drop was measured with a mercury manometer, while the test section pressure drop was measured with a small diaphragm type of pressure sensing element. This latter instrument requires a very small volumetric displacement for full scale reading. Thus once this system was filled with water there was never any danger of having a two-phase mixture in the connecting tubing. Both the pressure taps and the dye sampling taps were 1/16-in. diameter holes flush with the test section walls and located in the center of the 3-in. dimension.

Dye injection into the liquid film was accomplished by also introducing the colored liquid through porous plates, 0.0008 in. pore size, located 36 in. from the inlet. These plates were positioned on opposite sides of the channel and recessed so as to be flush with the inside surface. With this arrangement dye was introduced uniformly over the two 3-in. sides of the channel so that the condition of infinite width as assumed in the analysis was approximated. In order to maintain symmetry in the narrow direction of the channel the dye flow rates into each side of the channel were measured continuously and held equal. These rates were adjusted so that the dye flow rate was always less than 4% of the total flow in the liquid film. Dye concentrations were measured with a calibrated electrophotometer.

Total liquid volume fraction, or holdup, was measured with the rotating plug valve technique. These valves were made of brass and machined so that when full open their flow area matched exactly that of the Plexiglas channel. A system of levers joined each valve to a common mechanism so that both valves operated simultaneously and could be closed in less than 0.10 sec. A solenoid actuated pressure relief system was incorporated into the air and water piping so that these flows could be diverted to a drain when the plug valves were closed. Total liquid volume fraction was then found by simply measuring the height of water which collected on the top of the lower plug valve.

The velocity of the liquid film was determined by injecting a pulse of dye into the film and recording the output of two photocells as the colored water passed through their field

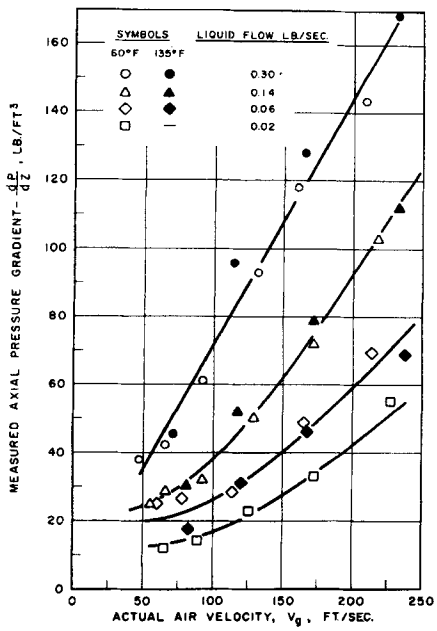

Fig. 3. Measured axial pressure gradient vs. actual air velocity.

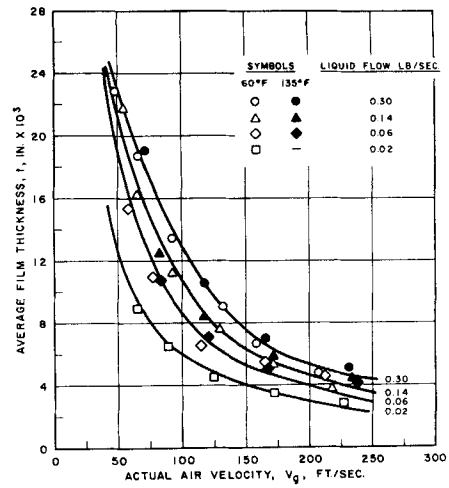

Fig. 4. Average film thickness vs. actual air velocity (film thickness computed assuming $V_D = V_G$).

of view. These detectors were located 4 ft. apart on the outside surface of the test section. The photocells were of the self-powered type, and their output was fed directly to two light-beam galvanometers in a visicorder. These signals were recorded on light sensitive paper and appeared as two broadening error curves. The distance between the two centers of concentration was used to compute the average transport time and thus the average velocity.

Experimental Results

The most striking feature of the vertical flow of air-water mixtures is the appearance of a definite wave pattern on the surface of the liquid film. At low air velocities the characteristic wave length is so long that possibly only one or two of these waves are in the channel at the same time. As the gas flow is increased to approximately 100 ft./sec. the wave length decreases so that many individual waves are in the channel at the same time. Simultaneously, the wave velocity increases, and their existence is detected by the visual observation of a significant amount of flickering of the flow field. At gas velocities near 200 ft./sec. the motion is so rapid that the flow now appears uniform to the eye. However, high-speed photographs show that waves are still present and that their length has decreased to the order of 1 in. Similar results are obtained for different liquid rates, the waves being more numerous at the higher liquid rates and virtually disappearing at the lowest liquid flows examined.

It is believed that these particular surface waves are similar to the roll waves described by Hanratty and Hershman (2).

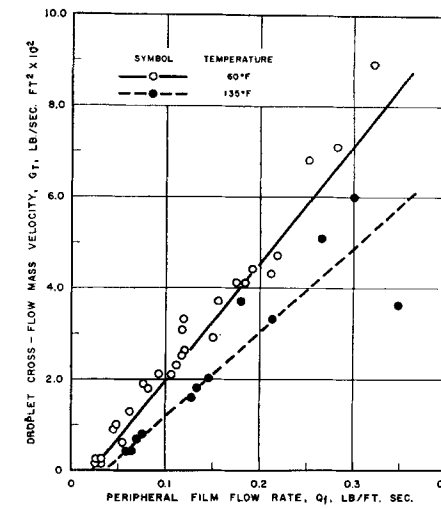

Fig. 5. Droplet cross-flow mass velocity vs. peripheral film flow rate.

However, they form in vertical flow and, from extrapolation to lower gas velocities, should be related to the liquid slugs found between vapor bubbles in a slug flow. (It may be postulated that the transition from slug flow to annular flow is accomplished by disrupting the liquid slug so that it becomes a long wave length wave.) High-speed motion pictures indicate that the principal cause of droplet formation is the atomization which occurs at the crests of these waves. Thus it seems that any analytical description of two-phase annular flow depends on an adequate understanding of these surface waves.

Table 1 presents the basic data obtained in this study. These data comprise five different liquid flow rates at room temperature and three liquid flow rates at 135°F. Each liquid rate was examined for a range of actual air velocities varying from 50 to 200 ft./sec. These same data are shown graphically in Figures 3 and 4 in which measured values of pressure gradient and liquid film thickness, respectively, are plotted vs. the actual air velocity. Figure 5 shows the measured droplet cross-flow mass velocity as a function of the peripheral film flow rate. All data evaluation was performed as described earlier.

It should be mentioned here that the reliability of these data is a strong function of gas velocity. Above about 100 ft./sec. it is felt that the assumed physical model adequately describes the true situation. However, at lower velocities, where there might only be one wave in the channel, all variables are subject to severe fluctuations, and interpretations based on the time and space averaged model of Figure 1 are questionable. Concerning the question of steady state it may be noted that the two-phase flow system studied herein was created somewhat abruptly at the bottom of the channel. It is reasonable to suppose that when wave processes are involved, an equilibrium condition will develop after perhaps five to ten wave lengths. Thus it is possible that the low velocity data, where there might be only one or two waves in the test channel, are not representative of fully developed flow. However, the higher velocity data should tend to reflect more of a steady state fully developed flow pattern. Hence in the following discussion reduced weight has been put on the low velocity data as compared with higher velocity effects.

DISCUSSION

As mentioned previously, the purpose of this study is to present and discuss a set of experimental data which describe in some detail the two-phase annular flow regime. It is not the purpose to develop new empirical correlations from this limited range of data, but instead to explore the physical nature of annular flow. Extrapolation of these results to other fluids and geometries is still uncertain because of the seeming importance of the surface waves, about which little is currently understood.

Effect of Temperature

Based upon the total pressure gradient data shown in Figure 3 it might be supposed that a factor of 2 change

Table 1. Experimentally Determined Average Parameters for Vertical Two-Phase Annular Flow in a 3- × ¼-in. Rectangular Channel

Data point number	Actual air velocity, V_g, ft./sec.	Air density, ρ_g, lb./cu. ft.	Water flow, W_l, lb./sec.	Liquid volume fraction, R_{lf}, cu. ft./cu. ft.	Axial pressure gradient, $-\frac{dp}{dz}$, lb./cu. ft.	Fraction of liquid entrained, E, lb./lb.	Cross-flow mass velocity, G_f, lb./sec.-sq. ft.	Film velocity, V_f, ft./sec.
			Part A, $T_g = 73°F.$, $T_L = 58°F.$					
1	207	0.088	0.295	0.045	143	0.72	0.037	11.2
2	159	0.086	0.293	0.062	118	0.68	0.041	10.2
4	92	0.082	0.300	0.122	61	0.62	0.043	7.4
6	48	0.080	0.294	0.205	38	0.41	0.089	4.2
7	230	0.087	0.224	0.048	124	0.71	0.026	8.4
8	181	0.085	0.212	0.063	101	0.70	0.031	8.5
10	100	0.081	0.213	0.110	49	0.70	0.033	6.4
12	50	0.079	0.215	0.240	29	0.29	0.071	4.0
13	218	0.085	0.127	0.034	103	0.67	0.019	7.8
14	171	0.083	0.122	0.048	72	0.59	0.021	6.6
15	129	0.081	0.136	0.068	50	0.56	0.023	5.7
17	66	0.080	0.131	0.143	29	0.38	0.029	3.3
19	211	0.083	0.052	0.041	70	0.50	0.010	4.4
20	166	0.081	0.049	0.048	49	0.50	0.009	3.6
21	114	0.080	0.056	0.058	29	0.48	0.006	3.0
23	57	0.079	0.055	0.133	26	0.20	0.018	1.3
24	226	0.081	0.020	0.024	55	0.16	0.002	3.0
25	171	0.080	0.022	0.030	33	0.23	0.002	2.7
26	125	0.079	0.022	0.039	23	0.20	0.002	2.0
28	65	0.078	0.024	0.077	12	0.14	0.002	0.7
			Part B, $T_g = T_L = 135°F.$					
29	231	0.076	0.302	0.047	170	0.62	0.033	15.0
30	165	0.074	0.306	0.064	128	0.53	0.051	11.0
31	117	0.071	0.308	0.094	96	0.39	0.036	8.9
33	233	0.072	0.162	0.039	112	0.56	0.018	11.5
34	171	0.070	0.140	0.052	79	0.51	0.016	8.5
35	117	0.068	0.144	0.074	52	0.45	0.020	6.7
37	238	0.070	0.060	0.038	69	0.47	0.004	5.0
38	167	0.068	0.060	0.045	46	0.44	0.004	4.6
39	120	0.068	0.061	0.062	31	0.39	0.007	3.8

in liquid viscosity has no effect upon the annular flow parameters. However, Table 1 shows that the film velocity increased noticeably with temperature, that the film thickness was unaffected, and that the entrainment decreased with an increase in temperature. At the same time Figure 5 shows the droplet cross-flow mass velocity to be lower at the higher temperatures. These data imply that as the liquid viscosity is decreased, the liquid film becomes more stable and the fraction of the total liquid flow in the film increases. Furthermore, the increased liquid film flow did not greatly alter the momentum transfer with the fast moving gas, since the total pressure gradient was unaffected by this redistribution.

Droplet and Film Velocities

It was expected that the axial droplet velocities could be calculated from the measured liquid fraction, film velocity, entrainment, and total liquid flow rate. When this was done the computed axial droplet velocities were much lower than the gas velocity and, in some cases, even lower than the film velocity reported in Table 1. This was surprising, since it was felt that the droplets moved at velocities close to that of the gas and that this procedure would provide some indication of the small amount of slip in the gas-droplet core. Hewitt, in a discussion of this paper, pointed out that the droplets could probably be assumed to move at the gas velocity, and that alternatively a film velocity could be calculated from the entrainment and liquid fraction. Surprisingly, this calculated film velocity was generally equal to one half of the measured value. Figure 6 is a plot of the measured film velocity vs. that calculated by assuming the droplets to move at the average gas velocity.

A review of the dye pulse technique for measuring the film velocity revealed that a large liquid pulse was required to obtain a visual signal from the photocells. This was in contrast to the entrainment measurements where the amount of dye injected was so small that it could not be observed visually. Therefore, the measured film velocity probably represented the velocity of a surge of liquid on top of the film. Returning to Figure 6, this indicates that surges, or possibly waves, move at twice the average film velocity. Whatever the true case, the measured values of film velocity are not felt to be reliable. Because of this the calculated film thicknesses shown in Figure 4 were based on the assumption that the entrained droplets travelled at the gas velocity.

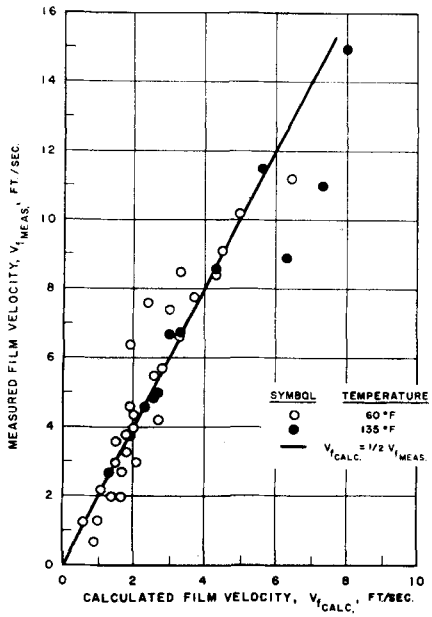

Fig. 6. Measured vs. calculated film velocity.

Film Properties

One rather fundamental property of a flowing film is the relationship between its thickness and flow rate. The total peripheral mass flow in the film is given by the integral

$$Q_f = \rho_f \int_0^t u\, d\, y \qquad (14)$$

In normal turbulent pipe flow it has been established that the flow in the vicinity of a solid surface is related to the distance from the surface by the dimensionless quantities u^+ and y^+. These parameters have been found to be applicable to a wide variety of conditions and are probably intimately related to the characteristic eddy patterns which develop in turbulent flow. The use of u^+ to describe film flow was first suggested by Dukler (*18*), and it has been applied with some success also by Lacey, Hewitt, and Collier (*19*). If the characteristic eddy sizes are thought of in terms of a Prandtl mixing length, then it might be expected that the same correlation would apply to both pipe and film flow, except near the film free surface where the eddys would be smaller for the film situation. The generalized $u^+ - y^+$ relation is readily related to film flows by substitution in Equation (14)

$$W^+ = \frac{Q_f}{\mu_f} = \int_0^{Y^+} u^+\, dy^+ \qquad (15)$$

which indicates that W^+, the dimensionless film flow, is a particular function of Y^+, the dimensionless film thickness. The integral in Equation (15) has been evaluated with the standard velocity profile data for pipe flow, and the resulting relationships between Y^+ and W^+ are shown in Figure 7. Also shown are the measured values of W^+ and Y^+. Here, W^+ is computed directly from the measured value of Q_f, while Y^+ is computed from the film thickness and the wall shear stress. It may be seen that the present data agree fairly well with the generalized velocity profile data. The film thicknesses, which are the most uncertain variables, may be interpreted to average about 30% higher than the theoretical values. Whatever the reason for the slightly higher Y^+ values, it appears that a knowledge of τ_w, Q_f, and μ_f are sufficient to obtain a good approximation to the film thickness. It should be pointed out that this treatment becomes unclear for $\tau_w < 0$. Such situations were not encountered in the present study.

A somewhat surprising result of this investigation was the behavior of the liquid film thickness. Figure 4 shows the film thickness to be relatively insensitive to the total liquid flow or viscosity and primarily dependent only upon the gas velocity. Thus, for an actual gas velocity of about 170 ft./sec., the film thickness remained in the range 3.5 to 7.0 $\times$ 10^{-3} in. for a factor of 10 change in the liquid flow. At the same time the film thickness (with $V_d = V_g$ assumed) appears to be approximately inversely proportional to the gas velocity. This variation is felt to be significant since it is directly related to the measured liquid fraction (the assumption that the droplets move at the gas velocity generally resulted in their volume fraction being negligible). Moreover, this result has a direct bearing on the calculation of the gross slip ratio through the following equation

$$U = \frac{V_g}{V_L} = \frac{V_g R_{1t} A_t \rho_f}{W_L} = \frac{V_g R_{1t}}{V_{LSup}} \qquad (16)$$

Since the gross slip ratio is dependent upon liquid fraction, which is in turn dependent upon film properties, it might

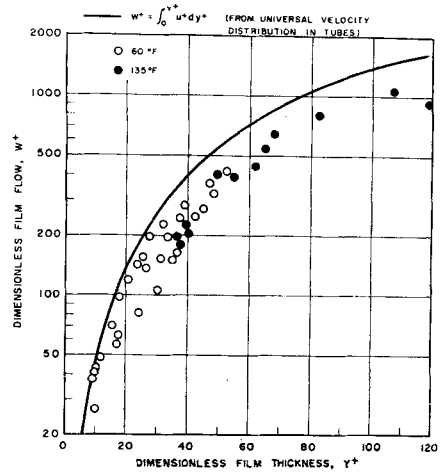

Fig. 7. Dimensionless film flow vs. dimensionless film thickness.

be concluded that the film turbulent hydrodynamics are of major significance in establishing the liquid fraction and slip ratio in annular flow. This is most evident at high gas velocities where the slow moving film has such a great effect on the slip ratio. In this regard, a large amount of consistent data has been reported by Govier (22) and his co-workers.

Core Properties

It may be recalled that a number of assumptions have been made concerning the nature of the gas-droplet core in order to develop the analytical procedure for evaluating the droplet transverse mass velocity. These assumptions allowed the core to be treated as having a uniform droplet dye concentration and constant axial gas and droplet velocities. Studies of the core by Adorni (23) and Hewitt (24) show that the droplet volume concentration is relatively constant across the core but that the velocity profiles are more peaked than in single phase turbulent flow. These two effects tend to move the entrained water to the center of the channel. This would not greatly alter the present approach if the transverse droplet mixing was very large. The mixing will be complete if the diffusional relaxation time of the droplets in the core is much smaller than say the transport time across the core at V_t. Hence it is necessary that the following criterion be met for a uniform core dye concentration to exist

$$\frac{a^2}{2D} << \frac{a}{V_t} \qquad (17)$$

If the diffusion coefficient is taken as the single phase value, $D \approx 0.5\ a \times V_g \times 10^{-2}$, then inequality (17) becomes the following

$$\frac{100\ V_t}{V_g} << 1 \qquad (18)$$

The measured transverse droplet velocities in this investigation were of the order of 0.2 ft./sec. Thus, it might appear that the criterion was met fairly well. However, there is evidence that heavy particles do not diffuse as rapidly as the lighter medium in which they are dispersed. For example, Soo, Ihrig, and El Kouh (25) have measured suspended particle diffusivities 1/50 that of the air stream. Evidently, future studies of two-phase annular flow should be designed to account for, and measure, droplet diffusion in the core. In the present case, the effect of poor droplet mixing in the core would be to make the calculated transverse mass velocities shown in Table 1 less than the true values.

It was pointed out earlier that the turbulent characteristics of the liquid film establishes the observed liquid fraction and slip ratio in the annular flow regime. The part played by the turbulent gas-droplet core is therefore to establish the frictional drag or pressure drop associated with this type of flow. Such must be the case since the high axial velocities associated with the core are continually transferred to the slowly moving film by turbulent mixing. Because the liquid film is relatively thin, the shear stress developed at the interface is transmitted almost unaltered to the stationary wall. Thus good transverse communication of axial momentum in the core brings high velocity fluid into close contact with the low velocity film and makes it more difficult for the core to flow. When one takes the measured droplet transverse mass velocities from Table 1, a resultant film-core shear stress may be computed as in Equation (12). The stress attributable to droplet interchange was thus found to vary from 0 to 30% of the total interfacial stress. The fractional droplet stress was highest at the highest water rates and appears relatively independent of gas velocity.

The final result of transverse momentum transfer is, of course, pressure drop, the overall process being described for single-phase flow by a friction factor defined in terms of the Reynolds number. Unfortunately, in two-phase flow the similarities implicit in the friction factor-Reynolds number relationship do not exist. This is to be expected since the heavier particles may not diffuse as rapidly as the gas phase (25). However, for many of the present conditions these same droplets account for the majority of the axial momentum in the core. Therefore, the transverse variation of the axial momentum in the core might be steeper than in the single phase case. From the above reasoning it appears possible that two-phase frictional losses might be less than those computed with a perfectly homogeneous mixture assumed. This conclusion is given some support by the core velocity profile data of Hewitt et al. (24), which indicate that the Prandtl mixing length constant is reduced from its usual value of 0.4 to 0.2 for a particular set of conditions. Nevertheless, while the core momentum diffusion constants may be less than for a homogeneous fluid, the increased drag associated with the wave roughness and the droplet transfer may act to increase the net momentum transferred, and thus the pressure drop, above the homogeneous values.

Film-Core Interactions

While the film and the core may be discussed separately and their respective characteristics treated independently, it is necessary to treat both regions simultaneously if two-phase annular flow is to be described analytically in its entirety. Thus the measured entrainment must represent an equilibrium situation between droplet deposition and wave breakup. Wave behavior and instability should be related to the $Y^+ - W^+$ characteristic along with the shear stress imposed by the core. At the same time droplet and gas transfer rates in the core are in part affected by the surface condition and in part by the concentration of liquid droplets. Thus analytical description of the complete process depends upon an understanding of the components as well as the peculiar interactions which they may have with each other. It is hoped that the present study has provided a more descriptive foundation upon which improved fundamental and empirical treatments of two-phase annular flow may be based.

CONCLUSIONS

1. Surface waves in the liquid film appear to dominate the gas-liquid hydrodynamics at low gas velocities. These

waves must be included in analytical models of low velocity annular flow.

2. Film surface waves in high-velocity flow appear to be small and uniformly distributed so that the physical model of two-phase annular flow shown in Figure 1 is reasonable. Nevertheless, their stability and interactions with the core must be better understood.

3. Waves or surges in the liquid film appear to travel at twice the average film velocity.

4. The average film flow rate and thickness appear to follow the dimensionless $Y^+ - W^+$ relationship established for single-phase pipe flow.

5. In two-phase annular flow the magnitudes of both the liquid volume fraction and the slip ratio seem to be influenced by the $Y^+ - W^+$ relationship in the film.

6. Droplet diffusion in the gas-droplet core is probably too small to justify the assumption made herein of a well-mixed core. Thus the droplet transverse mass velocities inferred from this study are probably lower than the true values.

7. For situations where the droplets account for a significant amount of the core axial momentum and mass flux the frictional resistance and mass transfer may be less than that of a homogeneous mixture of the phases.

ACKNOWLEDGMENT

The author wishes to express his appreciation to the U. S. Atomic Energy Commission, to the Westinghouse Electric Corporation, and to S. J. Green for the opportunity to perform this study and permission to publish these results.

NOTATION

A_t = total flow area of channel, sq. ft.
a = half the spacing between two parallel plates, ft.
C_f = dye concentration in the liquid film, lb./lb.
C_d = dye concentration in the liquid droplets, lb./lb.
C_m = bulk mixed dye concentration, lb./lb.
E = fraction of total liquid flow entrained as droplets, lb./lb.
G_d = droplet mass velocity in axial direction, lb./sec.-sq. ft.
G_t = cross-flow droplet mass velocity, lb./sec.-sq. ft.
k = droplet mass interchange coefficient, ft.$^{-1}$
L = channel width dimension, ft.
dp/dz = axial pressure gradient, lb./cu. ft.
Q_f = peripheral film flow, lb./ft.-sec.
R_{gt} = total gas volume fraction
R_{lt} = total liquid volume fraction
R_{gc} = actual gas volume fraction in core
t = thickness of liquid film, ft.
u = axial velocity at location y from the wall, ft./sec.
u^+ = dimensionless velocity, u/u^*
u^* = friction velocity, $\tau_w g/\rho_f$, ft./sec.
V_f = average velocity of liquid film, ft./sec.
V_g = actual average gas velocity, ft./sec.
V_L = effective axial liquid velocity, ft./sec., $V_L = \dfrac{W_l}{A_t R_{lt} \rho_f}$
V_{LSup} = superficial liquid velocity, ft./sec., $V_{LSup} = \dfrac{W_l}{A_t \rho_f}$
V_d = axial droplet velocity, ft./sec.
V_t = cross-flow droplet velocity, ft./sec.
W_g = total weight flow of gas, lb./sec.
W_l = total weight flow of liquid, lb./sec.
W^+ = dimensionless film flow, Q_f/μ_f
z = co-ordinate in the direction of flow, ft.
y = co-ordinate normal to the direction of flow, ft.
y^+ = dimensionless distance from the wall, $y^+ = \dfrac{yu^*\rho_f}{\mu_f}$
Y^+ = dimensionless film thickness, $Y^+ = \dfrac{tu^*\rho_f}{\mu_f}$
μ_f = viscosity of the liquid phase, lb./ft.-sec.
ρ_f = density of the liquid phase, lb./cu. ft.
ρ_g = density of the gas phase, lb./cu. ft.
τ_f = gas-liquid interfacial stress resulting from air drag on the liquid surface, lb./sq. ft.
τ_{ft} = total interfacial shear stress, lb./sq. ft.
τ_w = wall shear stress, lb./sq. ft.

LITERATURE CITED

1. Lighthill, M. J., *J. Fluid Mech.*, **14**, 385.
2. Hanratty, T. J., and A. Hershman, *A.I.Ch.E. Journal*, **7**, No. 3, 488 (1961).
3. Baker, O., *Oil and Gas J.*, **53**, 185 (1954).
4. Isbin, H. S., et al., "Two-Phase Steam-Water Pressure Drops," Preprint N. 147, Nuclear Engineering and Science Conference, Chicago, Illinois (1958).
5. Tippets, F. E., "Critical Heat Flux and Flow Pattern Characteristics of High Pressure Boiling Water in Forced Convection," *GEAP-3766* (Apr., 1962).
6. Sachs, P., and R. A. K. Long, *Int'l. J. Heat and Mass Trans.*, **2**, No. 3, 222 (1961).
7. Kinney, G. R., A. E. Abramson, and J. L. Sloop, *Natl. Advisory Comm. Aeronaut. Rept. 1087* (1952).
8. Isbin, H. S., R. Vanderwater, et al., *Trans. Am. Soc. Mech. Engrs.*, **83**, 149 (1961).
9. Goldman, K., et al., *ibid.*, 341.
10. Silvestri, M., "Two-Phase (Steam and Water) Flow and Heat Transfer," 1961 International Heat Transfer Conference, International Developments in Heat Transfer, Part II, p. 341 (1961).
11. Martinelli, R. C., and D. B. Nelson, *Trans. Am. Soc. Mech. Engrs.*, **70**, 695 (1948).
12. Collier, J. G., and G. F. Hewitt, "Data on the Vertical Flow of Air-Water Mixtures in the Annular and Dispersed Flow Regions," *AERE-R-3455* (1960).
13. Dukler, A. E., and P. G. Magiros, "Developments in Mechanics," Vol. 1, p. 352, Plenum Press, New York (1961).
14. van Rossum, J. J., *Chem. Eng. Sci.*, **11**, 35 (1959).
15. Bankoff, S. G., *Am. Soc. Mech. Engrs. Paper 59-HT-7* (1959).
16. Levy, S., "Prediction of Two-Phase Pressure Drop and Density Distribution from Mixing Length Theory," General Electric Atomic Power Equipment Department Report, *GEAP-3268*, Revision 1 (1961).
17. Calvert, S., and B. Williams, *A.I.Ch.E. Journal*, **4**, 78 (1958).
18. Dukler, A. E., *Chem. Eng. Progr. Symposium Ser. No. 30*, **56**, 1 (1960).
19. Lacey, P. M. C., G. F. Hewitt, and J. G. Collier, "Climbing Film Flow," *AERE-R-3962* (1962).
20. "A Study of Wet Steam as a Reactor Collant," Joint Report by CISE, Ansaldo and NDA, *CISE Rept. R-44* (NDA-2132-6) (1961).
21. Wicks, M., and A. E. Dukler, *A.I.Ch.E. Journal*, **6**, No. 3, p. 463 (1960).
22. Govier, G. W., R. A. S. Brown, and G. A. Sullivan, *Can. J. Chem. Eng.*, **38**, 62 (April, 1960).
23. Adorni, N., et al., "Experimental Data on Two-Phase Adiabatic Flow: Liquid Film Thickness, Phase and Velocity Distribution, Pressure Drops in Vertical Gas-Liquid Flow," *CISE Rept. R-35* (March, 1961).
24. Hewitt, G. F., L. E. Gill, and J. W. Hitchon, "Sampling Probe Studies of the Gas Core in Annular Two-Phase Flow," *AERE-R-3954* (November, 1962).
25. Soo, S. L., H. K. Ihrig, Jr., and A. F. El Kouh, *Am. Soc. Mech. Engrs. Paper No. 59-A-59* (1959).

Manuscript received January 15, 1963; revision received December 14, 1964; paper accepted December 16, 1964. Paper presented at A.I.Ch.E. Chicago meeting.